Progress In Electromagnetics Research C, Vol. 65, 111–119, 2016

Dual Notch UWB Fork Monopole Antenna with CRLH Metamaterial Load

Zahra Mansouri[1], Afsaneh Saee Arezomand[2], Samaneh Heydari[3], and Ferdows B. Zarrabi[4, *]

Abstract—A novel fork monopole antenna is presented using metamaterial structures. The prototype monopole antenna consists of split-ring-resonators (SRR) as an electric-LC resonator and small ground. To prove the concept, the prototype antenna is designed and fabricated for wireless communication systems. The monopole structure makes ultra wideband (UWB) impedance bandwidth condition for 2–12 GHz. On the other hand, the prototype antenna shows dual notch band characteristics at 3.5–4.5 GHz and 5.3–6 GHz for WiMAX and WLAN rejection. The prototype antenna radiates omnidirectionally and has a gain altered between −4.5 and 6.2 dBi in 2.5–12 GHz, with an average gain of 4.2 dBi. The metamaterial model is suggested for the CRLH (ELC) resonator, and in addition, the parametric study for CRLH (ELC) resonator is presented for clarification of its manner on resonance controlling. Here, the final model antenna is fabricated on an FR-4, and experimental results are compared with simulations.

1. INTRODUCTION

Over the last decade, many applications of wireless communication systems have been proposed, such as radar, medical field and personal communications and portable devices such as notebooks and cellular phones with low profile and low cost condition [1, 2]. Among these applications, UWB antennas are very important devices for high speed rates, low cost, low power wireless systems and broadband usage [3, 4]. The Federal Communications Commission (FCC) allowed application of the frequency band 3.1 to 10.6 GHz for UWB systems [5]. On the other hand, various applications of UWB communication systems exist in different frequency bands, such as 5.15–5.825 GHz for Wireless Local Area Network (WLAN), 5.25–5.85 GHz for Worldwide Interoperability for Microwave Access (WIMAX), and notch band antenna are noticed and used as a multiband antenna for the avoidance of electromagnetic interference with IEEE 802.11a standard for 5.15–5.35 GHz [6, 7]. The planar monopole antennas are important components for the UWB communication systems because of their simple structure, low profile, low cost, easy fabrication, and impedance matching. Finally, these advantages make the planar monopole antennas attractive for implementation at UWB applications [7, 8]. Various types of printed monopole antennas have been designed for UWB applications. A fork-shaped radiating patch with an inverted T-shape parasitic [9] structure, a G-shaped slots ground plane and a small square monopole antenna with an inverted T-shaped slot and conductor-backed plane with different shapes such as Ω and Γ are used for enhancement of antenna bandwidth and making notches band characteristic [9, 10]. Fork shaped antenna with different formations and parasitic elements such as L-shaped conductor-backed elements are used for UWB applications [11, 12]. Microstrip slot antennas with different slot shapes, e.g., T-shape [13], H-shape [14], U-shape and L-shape [14] used to obtain the favorable frequency band notch, have been studied. In addition, fractal and parasitic structures are usual approaches for generating multiple band

Received 7 April 2016, Accepted 12 June 2016, Scheduled 26 June 2016

* Corresponding author: Ferdows B. Zarrabi (ferdows.zarrabi@yahoo.com).

[1] Young Researchers and Elite Club, Abhar Branch, Islamic Azad University, Abhar, Iran. [2] Young Researchers and Elite Club, Urmia Branch, Islamic Azad University, Urmia, Iran. [3] Department of Electrical Engineering, Isfahan (Khorasgan) Branch, Islamic Azad University, Isfahan, Iran. [4] Young Researchers and Elite Club, Babol Branch Islamic Azad University, Babol, Iran.

notched antennas based on CPW or other UWB structures [15]. Metamaterials structures such as Split Ring Resonator (SRR), Zeroth order resonators (ZOR) and CRLH transmission line because of negative effective permittivity and permeability are noticed for different applications such as phase changing [16], miniaturization [17] and multi-notches applications [18]. Also capacitance loaded loop (CLL) resonator, magnetic and electric-LC resonators and electric LC element, and EBG resonator are used for making notches resonance and act as SRR structures [19–21]. An equivalent circuit for a CRLH transmission line is shown in Fig. 1. According to this figure, the CRLH-TL includes series inductors and parallel capacitors, also includes parallel inductors and series capacitors. Series inductor and parallel capacitor are known as right-handed TL (L_R and C_R), and a parallel inductor and series capacitor are called left-handed inductor and capacitor (L_L and C_L). Achieving a structure with left-handed features is nearly impossible [22, 23].

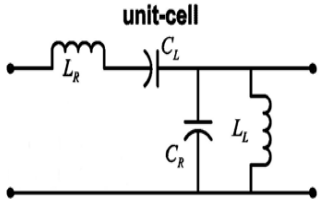

Figure 1. An equivalent circuit for a CRLH transmission line.

Effective permeability and permittivity for metamaterial transmission line (MTL) can be achieved by calculation of Z' and Y' as presented in Eq. (1) [24, 25]:

$$\mu = \mu(\omega) = L_R - \frac{1}{\omega^2 C_L} = \frac{Z'}{j\omega} \quad \varepsilon = \varepsilon(\omega) = C_R - \frac{1}{\omega^2 L_L} = \frac{Y'}{j\omega} \tag{1}$$

where

$$Z' = j\left(\omega L_R - \frac{1}{\omega C_L}\right)\ \Omega/m \quad Y' = j\left(\omega C_R - \frac{1}{\omega L_L}\right)\ S/m \tag{2}$$

The phase velocity and group velocity of CRLH-TL structure can be parallel or anti-parallel, depending on the operating frequency. In this structure, there is a frequency that separates the left-handed region from the right-handed one. We call it transmission frequency and calculate it by the following equation [24]:

$$\omega_0 = \sqrt{\omega_R \omega_L} = \frac{1}{\sqrt[4]{L_R C_R L_L C_L}} \tag{3}$$

Therefore, the dispersion relation for the homogeneous CRLH-TL is:

$$\gamma = \alpha + j\beta = jS(\omega)\sqrt{\left(\frac{\omega}{\omega_R}\right)^2 + \left(\frac{\omega_L}{\omega}\right)^2 - k\omega_L}, \quad k = C_R L_L + C_L L_R \tag{4}$$

where $S(\omega)$ has the following sign function:

$$S(\omega)\begin{cases} -1 & \text{if LH range} \\ +1 & \text{if LH range} \end{cases} \tag{5}$$

In this paper, the design of a new fork monopole antenna using a split ring resonator (ELC) along with small ground plane is proposed for the achieved dual notch-band characteristic. The prototype antenna has two rejection bands at 3.5–4.5 GHz and 5.3–6.2 GHz. The experimental and simulated results are compared, and the antenna voltage standing wave ratio (VSWR) shows the effect of the CRLH or ELC resonator on antenna rejection.

2. ANTENNA STRUCTURE

Figure 2 illustrates the geometry of the prototype UWB antenna. The monopole structure is similar to the fork models, and the antenna is composed of a meandered shape as a top layer and a small

ground plane with CRLH unit cell (electric-LC element) at the bottom of the substrate. Here, the ELC resonator and CRLH unit cell placement and their coupling with the monopole element have a great impact on the notch frequency and bandwidth of the antenna. This placement is noticed for the rejection band at WLAN and WiMAX applications, and ELC is investigated for multi-band applications [21]. In addition, a 50 Ω subminiature version A (SMA) is connected to the patch for excitation of the antenna by a microstrip line. The dimension of each part of the antenna is given in Table 1. The prototype antenna is fabricated on a low cost FR-4 substrate with $\varepsilon_r = 4.4$, and the fabricated antenna is shown in Fig. 2(c). Fig. 2(d) shows the capacitance (C_1 and C_2) and inductance (L) in the proposed resonator. As shown here, the gaps provide capacitance properties while the strips act as inductors.

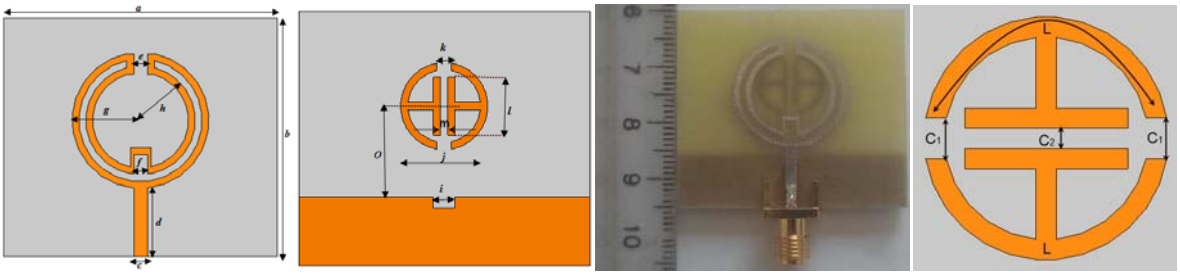

(a) (b) (c) (d)

Figure 2. The geometry of the prototype antenna and fabricated model. (a) Top layer of a monopole antenna (fork antenna). (b) Bottom layer of the antenna (the ground and ELC resonator). (c) The fabricated antenna. (d) The proposed electric-LC resonator.

Table 1. Geometry of the prototype antenna.

Parameter	mm	Parameter	mm
a	40	h	8
b	35	i	3
c	2	j	12
d	10	k	2
e	2	l	8
f	2	m	1
g	10	o	12.5

3. SIMULATION AND EXPERIMENTAL RESULTS

The antenna VSWR is shown in Fig. 3. In Fig. 3(a) we present a comparison between the fork antennas with the presence and absence of ELC-load unit cell. The fork antenna has a notch resonance at 5.3–6 GHz, and when the CRLH unit cell (ELC resonator) is added to the structure, another notch frequency appears in the range of 3.5–4.5 GHz with any effect on the second notch band of the antenna. The prototype structure works as a multi-band antenna in the frequency range 2.5–12 GHz. Fig. 3(b) shows the simulated VSWR in good agreement with the measurement results. The simulations are performed using HFSS software, and the measurement is done using HP8722ES network analyzer. The prototype antenna shows the dual notch band characteristic at 3.5–4.5 GHz and 5.3–6 GHz for WiMAX and WLAN rejection.

Fig. 4 shows the efficiency of the prototyped UWB antenna, which is obtained by HFSS, and it is typically over 70%. The antenna efficiency is decreased dramatically at notch bands as shown here. At the first notch, efficiency is reduced to about 20% for 4.2 GHz. At the second notch frequency, the antenna efficiency is reduced to 42% at 5.5 GHz. On the other hand, at lower frequency, the VSWR is increased more than 2, so the efficiency is reduced to 35%.

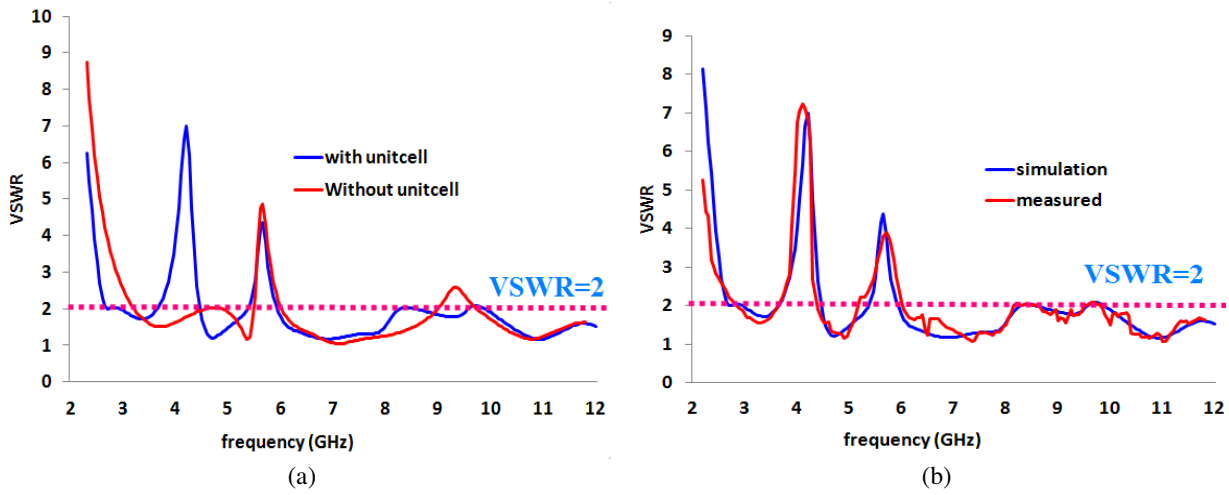

Figure 3. VSWR comparison. (a) Fork antenna in presence and absence of ELC resonator (Unit Cell). (b) The simulation and experimental result.

The antenna gain in the range of 2–12 GHz is between −4.5 dBi and 6.2 dBi as shown in Fig. 5, and simulated and measured results are compared. The negative value of antenna gain in the frequency range of 2–2.6 GHz is because of high VSWR and mismatching at lower frequency.

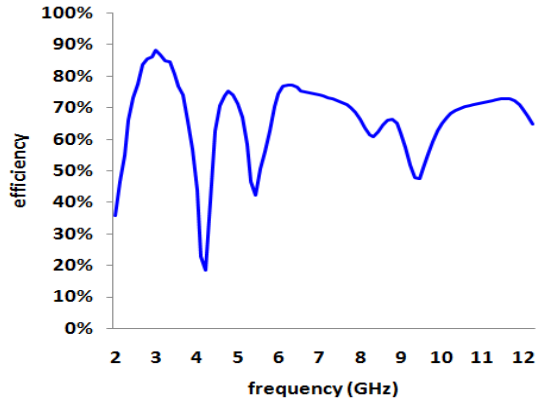

Figure 4. Efficiency simulated with HFSS.

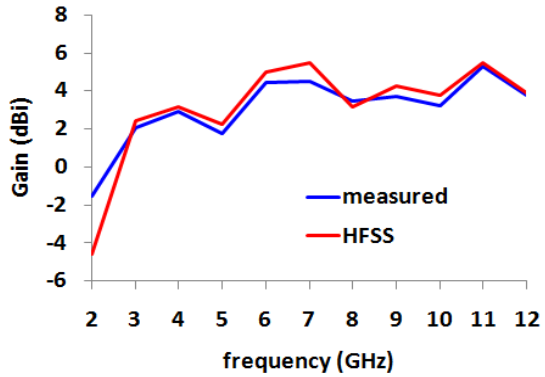

Figure 5. Simulated and measured of antenna gain.

Fig. 3(a) shows the effect of CRLH (ELC resonator) on the first notch frequency. For adjusting the impedance matching of a band-rejection, the effect of the ELC resonator placement on antenna VSWR is presented at Fig. 6. Accordingly, we simulated the VSWR of the antenna for the various offset values of the CRLH unit cell from the ground ('O' in Fig. 2(b)). In the first case, the CRLH is adjacent to the ground plane, and the result is shown in Fig. 6(a). In the second case, CRLH is moved to the upper part, and results are presented at Fig. 6(b). In both cases, the antenna notch quality is reduced, and the notch frequencies are shifted to the higher frequency. By moving CRLH to upper places with steps of 1 mm, the coupling from the monopole element (fork antenna) on CRLH is reduced, and the omission of the first notch is predictable as 4 mm and 5 mm offsets at Fig. 6(b). Therefore, the current placement of CRLH gives us the best notch band frequency.

As shown in this paper, the first and second notches are made by metamaterial load and fork structure, respectively. In the metamaterial unit cell, the gap provides the capacitance effect, and the loop strip is used to make the inductive effect of the ELC-load. Therefore, in order to realize the effect

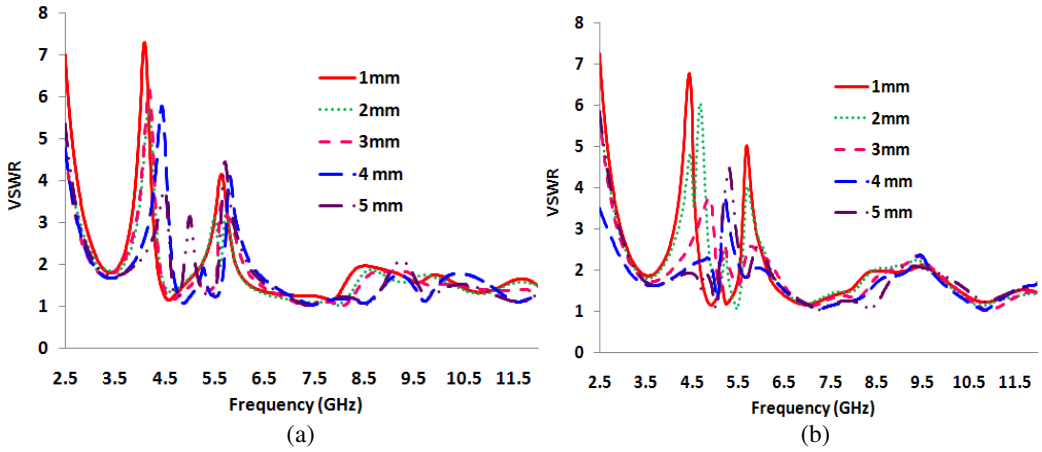

Figure 6. The placement offset of ELC resonator, (a) movement ELC resonator to down, (b) movement ELC resonator to up.

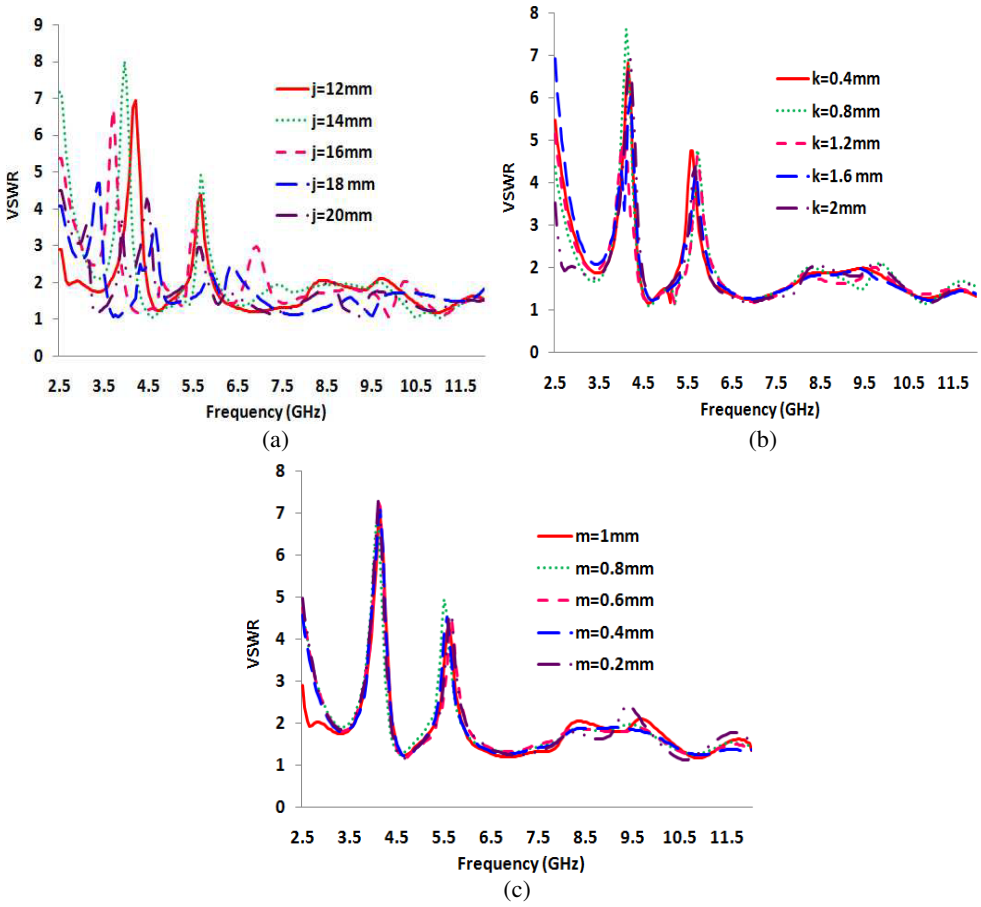

Figure 7. The CRLH (ELC-resonator) unit cell parameter effect on antenna resonance. (a) The unit cell radius effect. (b) The outer gap effect. (c) The inner gap effect.

on the resonant frequencies and impedance matching (VSWR) of corresponding structural parameters, a parametric study has been carried out. As illustrated in Fig. 7, by varying j, k and m, and fixing other parameters, the second resonance changes slightly, which indicates that the effect of the ELC-load on the original resonant frequency of the fork monopole part is small. By increasing the radius of the

unit cell, the inductance will increase, and the first resonance decreases as shown in Fig. 7(a). The coupling of the fork monopole part of CRLH (ELC-load) unit cell is altered by increasing the size of the unit cell, so it causes alteration at the second resonance. Figs. 7(b) and 7(c) show the effects of the gaps on antenna notch resonance. In our proposed unit cell, we use two different gaps, indicated by C1 and C2 at Fig. 2(d). By changing (k), C1 will alter, and C2 will change by the gaps between two parallel parts of the CRLH (ELC-load). Both of these changes influence the lower frequency, and by reducing the capacitance properties, the bandwidth of the antenna between 2.5–3 GHz will be reduced drastically. More precisely, according to Fig. 7(a), the value of j varies from 12 to 20 mm with steps of 2 mm while the values of k and m maintain at 0.4 and 1 mm, respectively. The first resonance decreases with the increase of (j). With k increasing from 0.4 to 2 mm with steps of 0.2 mm as well as the value of j and m kept at 12 and 1 mm, the first and second resonances change negligibly, shown in Fig. 7(b). Also, with altering (m) from 0.2 to 1 mm with steps of 0.2 mm while the values of (j) and (k) maintain at 12 and 0.4 mm, the first and second notches change slightly, shown in Fig. 7(c). Thus, by changing these parameters, the resonant frequency can be adjusted to the requirement.

Figure 8 shows the surface current distribution simulations in HFSS 11 for three frequencies of 4, 5.7, 7 GHz. The current distribution for 4 GHz is shown in Fig. 8(a). As demonstrated here, the maximum current concentrates in the inner circle of the fork part and CRLH (ELC-load element), so at this frequency, the coupling of the monopole part of CRLH load is more than that in higher frequency. By increasing the frequency, the maximum current is shifted to the outer circle of the fork antenna, and the coupling is reduced on ELC-load element. Also in Fig. 8(b) for 5.7 GHz, the maximum current is observed in the outer circle. As shown in Fig. 8(c), the current distribution at 7 GHz is minimized at

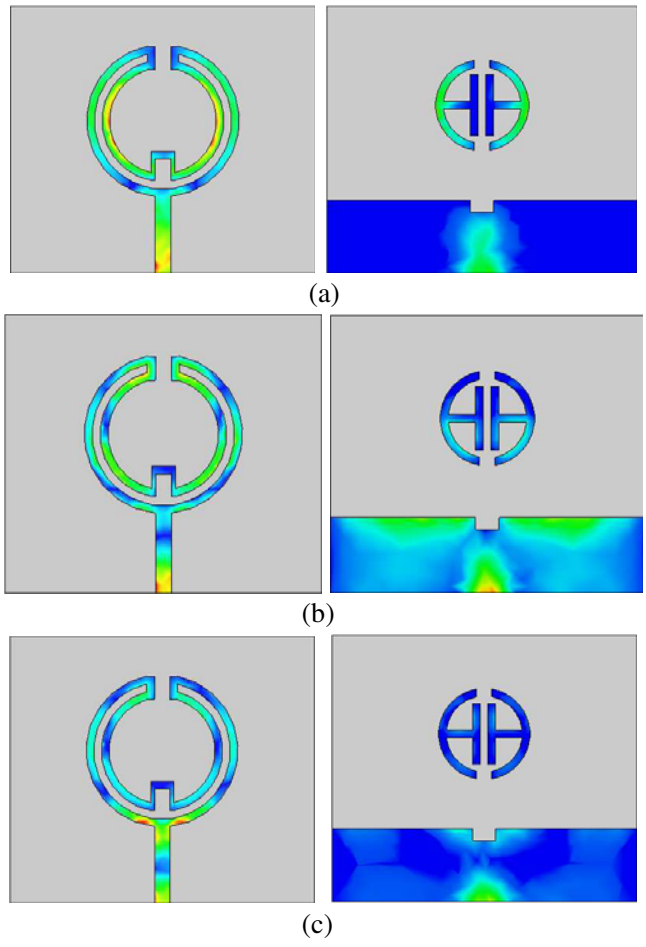

Figure 8. The antenna current distribution, (a) 4 GHz, (b) 5.7 GHz, (c) 7 GHz.

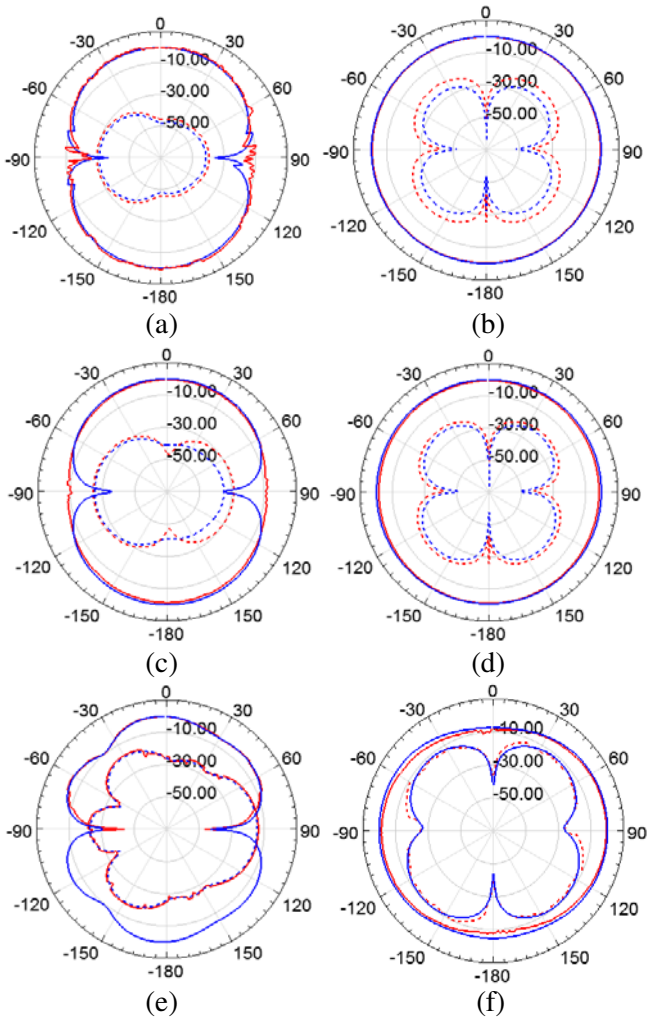

Figure 9. The simulated and measured radiation patterns of the proposed antenna (red-line for experimental). (a) H-plane at 3 GHz. (b) E-plane at 3 GHz. (c) H-plane at 4.5 GHz. (d) E-plane at 4.5 GHz. (e) H-plane at 7 GHz. (f) E-plane at 7 GHz.

ELC-load in this frequency, so it has no effect on the resonance at this frequency. In conclusion, we can realize that the coupling of the fork antenna on CRLH causes the first notch.

The measured radiation pattern (co-polarization and cross-polarization) in E-plane (y-z plane) and H-plane (x-z plane) at 3, 4.5 and 7 GHz of the prototype antenna is shown in Fig. 9 by the test in chamber room. It can be seen that the simulated results are in good agreement with measured ones. The antenna radiates omnidirectionally in the E-plane and approximately bi-directionally in the H-plane. The cross polarization is increased by increasing the operating frequency in E-plane.

4. CONCLUSION

In this article, a novel design of printed monopole antenna with electric-LC resonator and meander slot model is proposed, which operates from 2 to 12 GHz with two rejection bands near 3.5–4.5 GHz and 5.3–6 GHz. To validate the proposed results, a prototype antenna is designed, constructed and measured. A small ground plane is used to improve the impedance bandwidth of the antenna, and ELC resonator is applied. The simulated and experimental results show that this antenna can be a good selection of UWB systems.

REFERENCES

1. Boney, M., S. K. A. Rahim, R. Dewan, and B. M. Sa'ad, "Dual band trapezoidal antenna with partial ground and meander line feed for GPS and WiMAX applications," *Microwave and Optical Technology Letters*, Vol. 56, No. 2, 497–502, 2014.
2. Jiang, W. and W. Che, "A novel UWB antenna with dual notched bands for WiMAX and WLAN applications," *IEEE Antennas and Wireless Propagation Letters*, Vol. 11, 293–296, 2012.
3. Saee Arezoomand, A., R. A. Sadeghzadeh, and M. Naser-Moghadasi, "Investigation and improvement of the phase-center characteristics of VIVALDI's antenna for UWB applications," *Microwave and Optical Technology Letters*, Vol. 58, No. 6, 1275–1281, 2016.
4. Brar, R. S., S. Singhal, and A. K. Singh, "Fractal dipole antenna for UWB applications," *Microwave and Optical Technology Letters*, Vol. 58, No. 1, 39–47, 2016.
5. Choe, H. H. and S. J. Lim, "Ultrawideband compact U-shaped antenna with inserted narrow strip and inverted T-shaped slot," *Microwave and Optical Technology Letters*, Vol. 56, No. 10, 2265–2269, 2014.
6. Yang, L., Y. H. Cui, and R. L. Li, "A multiband uniplanar antenna for LTE/GSM/UMTS, GPS, and WLAN/WiMAX handsets," *Microwave and Optical Technology Letters*, Vol. 57, No. 12, 2761–2765, 2015.
7. Naser-Moghadasi, M., T. Sedgee, and C. Yekan, "Semifractal antenna with dual-bands filtering and circular polarization properties using SCBP and MDGS structures," *Microwave and Optical Technology Letters*, Vol. 57, No. 11, 2483–2487, 2015.
8. Mardani, H., C. Ghobadi, and J. Nourinia, "A simple compact monopole antenna with variable single-and double-filtering function for UWB applications," *IEEE Antennas Wireless Propagation Letter*, Vol. 9, 1076–1079, 2010.
9. Ojaroudi, M. and Y. Ojaroudi, "Band-notched low profile monopole antenna with enhanced bandwidth by using an inverted T-shaped parasitic structure and a pair of G-shaped slots," *Microwave and Optical Technology Letters*, Vol. 54, No. 5, 1123–1127, 2012.
10. Ojaroudi, N. and M. Ojaroudi, "G-shaped monopole antenna with dual band-stop function for UWB communications," *M, 2012icrowave and Optical Technology Letters*, Vol. 55, No. 11, 2686–2689, 2013.
11. Xu, P., Z.-H. Yan, and C. Wang, "Multi-band modified fork-shaped monopole antenna with dual L-shaped parasitic plane," *Electronic Letter*, Vol. 47, No. 6, 364–365, 2011.
12. Mishra, S. K., R. Kumar Gupta, A. Vaidya, and J. Mukherjee, "A compact dual-band fork-shaped monopole antenna for bluetooth and UWB applications," *IEEE Antennas Wireless Propagation Letter*, Vol. 10, 627–630. 2011
13. Zhang, S., B. K. Lau, Y. Tan, Z. Ying, and S. He, "Mutual coupling reduction of two PIFAs with a T-shape slot impedance transformer for MIMO mobile terminals," *IEEE Transactions on Antennas and Propagation*, Vol. 60, No. 3, 1521–1531, 2012.
14. Barbarino, S. and F. Consoli, "UWB circular slot antenna provided with an inverted-l notch filter for the 5 GHz WLAN band," *Progress In Electromagnetics Research*, Vol. 104, 1–13, 2010.
15. Naser-Moghadasi, M., R. A. Sadeghzadeh-Sheikhan, T. Sedghi, T. Aribi, and B. S. Virdee, "UWB CPW-fed fractal patch antenna with band-notched function employing folded T-shaped element," *IEEE Antennas Wireless Propagation Letter*, Vol. 12, 504–507, 2013.
16. Khaleel, H. R., H. M. Al-Rizzo, and D. G. Rucker, "Effects of bending on the performance of split ring resonators," *Microwave and Optical Technology Letters*, Vol. 54, No. 9, 2098–2101, 2012.
17. Bilotti, F., A. Alu, and L. Vegni, "Design of miniaturized metamaterial patch antennas with-negative loading," *IEEE Transactions on Antennas and Propagation*, Vol. 56, No. 6, 1640–1647, 2008.
18. Haroon, S., K. S. Alimgeer, N. Khalid, B. T. Malik, M. F. Shafique, and S. A. Khan, "A low profile UWB antenna with triple band suppression characteristics," *Wireless Personal Communications*, Vol. 82, No. 1, 495–507, 2015.

19. Kim, C., X. Cheng, D. E. Senior, and Y.-K. Yoon, "Compact frequency and bandwidth tunable stopband filters using split ring resonators and varactors coupled transmission line," *AEU-International Journal of Electronics and Communications*, Vol. 66, No. 11, 865–870, 2012.
20. Naqui, J., M. Duran-Sindreu, and F. Martin, " Differential and single-ended microstrip lines loaded with sloted mgnetic and electric-LC resonators," *International Journal of Antennas and Propagation*, 1–8, 2013.
21. Li, K., C. Zhu, L. Li, Y.-M. Cai, and C.-H. Liang, "Design of electrically small metamaterial antenna with ELC and EBG loading," *IEEE Antennas and Wireless Propagation Letters*, Vol. 12, 678–681, 2013.
22. Zarrabi, F. B., M. Rahimi, Z. Mansouri, and I. A. Lafmajani, "Miniaturization of microstrip antenna by CRLH-TL technique," *Wireless Personal Communications*, Vol. 81, No. 3, 1091–1100, 2015.
23. Ha, J., K. Kwon, Y. Lee, and J. Choi, "Hybrid mode wideband patch antenna loaded with a planar metamaterial unit cell," *IEEE Transactions on Antennas and Propagation*, Vol. 60, No. 2, 1143–1147, 2012.
24. Park, J.-H., Y.-H. Ryu, J.-G. Lee, and J.-H. Lee, "Epsilon negative zeroth-order resonator antenna," *IEEE Transactions on Antennas and Propagation*, Vol. 55, No. 12, 3710–3712, 2007.
25. Fashi, A. A., M. Kamyab, and M. Barati, "A microstrip small-sized array antenna based on the meta-material zeroth-order resonator," *Progress In Electromagnetics Research C*, Vol. 14, 89–101, 2010.